Deflagration and Detonation in Solid-Solid Combustion

Hendrik J. Viljoen
Dept. of Chemical Engineering, University of Nebraska-Lincoln, Lincoln, NE 68588

Vladimir Hlavacek
Dept. of Chemical Engineering, State University of New York at Buffalo, Amherst, NY 14260

Solid-solid combustion becomes self-sustaining when the preheating of the fresh mixture is high enough to support a spontaneous chemical reaction. These reactions have high activation energies, requiring significant preheating. Traditionally, conduction has been considered as the main form of preheating, and propagation velocities in the order of a few mm to a few cm per second were found. When acoustic equations are included in the analysis, no significant changes occur for traditional SHS reactions. However, the analysis of a 1-D model propagating at a constant velocity reveals the existence of two other solutions with propagation velocities which are much faster. An SHS deflagration wave is found with combustion temperature lower than the adiabatic value. The propagation velocity is less than the longitudinal sound speed of the medium, but typical Mach numbers vary between 0.6 and 0.95. The third solution is an SHS detonation with temperature above the adiabatic value and supersonic propagation velocity. Since the heat fluxes are extremely high, the hyperbolic conduction model is used.

Introduction

Fast solid-solid reactions represent an area of reaction kinetics which is both very important and poorly understood. If the solid-solid reaction is strongly exothermic, we can expect a rich spectrum of new physical phenomena. Since heat generation of solid-solid reaction can easily reach parameter values typical for explosive materials, we can contemplate phenomena of solid-solid detonation.

Enikolopyan (1989) published an article on super-fast chemical reactions in solids. His findings are based on experimental work done with a variety of materials in a Bridgeman anvil. Wafers of solid material were placed in a die and longitudinally or shear loaded. Reactions occur at extremely high rates, with little or no release of the heat of reaction. In one instance hydrated copper sulfate was mechanically activated and after a fast decomposition reaction, elemental copper was found in the die. In another article by Enikolopyan et al. (1991) the results of the decomposition of ammonium dichromate was reported. The adiabatic temperature rise for this reaction is 1,300°C, but they only measured temperature rises in the order of 300°C. 80% of the available chemical energy was used to support an elastic shock wave that propagated through the sample at a speed of $\approx$ 2,200 m/s. The reaction front lagged the shock wave, but it still propagated at a velocity of 1,300 m/s. They provide several other examples as evidence that chemical energy is not necessarily released in the form of heat. Enikolopyan also found that the critical mechanical load to initiate the fast reaction, depends on the wafer thickness. As the wafer thickness increases, the critical load decreases and there exists a minimum wafer thickness below which mechanical activation does not occur. These results underscore our lack of understanding of solid-phase chemical reactions.

Solid-phase reactions also do not follow Arrhenius rate dependence under all conditions. This experimental observation points to a change in the activation energy of a solid-solid system when it is compressed. The lowering of the activation energy makes the mixture more reactive and reaction can start at lower pre-heating. Benderskii et al. (1989) addressed this question of "activation" of a solid-phase reactive species by either thermal or mechanical means. To study the latter phenomenon, mechanical activation was studied for reacting

Correspondence concerning this article should be addressed to H. J. Viljoen.

mixtures at temperatures below 60 K. They advanced the following hypothesis

$$E = E_o - \alpha \Pi$$

where α is a dimensionless coefficient near unity and Π is the elastic potential energy (J/m^3) of the mixture. When a mixture is compressed, the elastic potential energy is increased and the global activation energy is decreased. (Tensile loading is nonsensical due to the low strain-to-failure of brittle materials.) If $\alpha \Pi = E_o$, the reaction will become perfectly spontaneous at the prevailing conditions.

Knyazeva and Dyukarev (1995) used the reduction of activation energy by mechanical loading to model the problem of steady-state propagation. They found four different propagation velocities, counting the kinetically controlled solution. A second solution is the typical SHS reaction, but the other two are subsonic and supersonic propagating states. Knyazeva (1993) also did a stability analysis of the deflagration and detonation solutions and found oscillatory instabilities when the stability threshold of the bifurcation parameter is exceeded. This result is not surprising, since the problem is quite similar to the traditional SHS problem. Sivashinsky (1981) showed that SHS propagation can be destabilized and a variety of new modes can develop which are associated with two- and three-dimensional spatial structures. It is therefore highly likely that symmetry breaking can occur in SHS deflagration and detonation.

In another series of experiments, Nesterenko and coworkers used an explosive to collapse copper cylinders filled with Mo + Si powders, Ti + Si, Nb + Si, and so on. The average particle sizes of the powders which were used in these experiments were more than 1 μm. Nesterenko et al. (1994, 1995) studied the structure of the reactive porous powders after compression by an explosive. Particle melting, changes in morphology and partial reaction have been observed. High shear rates are encountered during the explosion, causing the more malleable powders to deform into thin parallel layers. This results in an increase in the contact area between reactants. Inside the shear bands vortices formed. A numerical study of this process was done by Benson et al. (1995). The focus of their work was on the effects of high strain rates on the mechanical, physical and to a lesser extent chemical properties of a mixture of reactive powders.

Using the Frank-Kamenetskii equation for the velocity of solid-flame propagation, we can estimate for fine powders combustion propagation velocities in the range of several mm to tens of cm per second. This calculation is in agreement with experimental observations. For instance, for a conventional solid-solid reaction $Ti + C \rightarrow TiC$, the heat flux is in the range of $q \approx 10^4$ W/cm^2. However, for ultrafine powders which are mixed on the "micro-to-nano" level, diffusion resistance of solid-solid reactions is suppressed and the propagation velocities of the SHS deflagration is in the range 10–800 m/s (Danen and Martin, 1993; Taylor and Martin, 1991; Aumann et al., 1995). This will increase the heat flux to values of $q \approx 10^6$–10^8 W/cm^2. Eventually for a detonation SHS regime, the propagation velocities can be in the range of 4–10 km/s (Gogulya et al., 1991, 1992; Kovalenko and Iranov, 1981). The values of the heat flux can be 10^9–10^{10} W/cm^2. For comparison purposes, the oxy-acetylene flame provides a heat flux of $q \approx 10^3$ W/cm^2 and a powerful electron beam and laser 10^6 W/cm^2. At heat fluxes of the order of 10^7 W/cm^2 or greater, hyperbolic heat conduction becomes significant (Maurer and Thompson, 1973). Shlensky and Murashov (1983) studied exothermic chemical reactions which release energy at rates that cause the breakdown of the parabolic heat-transfer description and warrant the use of thermal inertia, a concept that was advanced by Morse and Feshbach (1953) and Boley (1964).

There is a growing body of experimental evidence that solid-solid combustion waves can couple with elastic waves to produce very high propagation velocities. There exists a synergism between thermoelasticity and chemical activation. Reactions can support elastic waves, and elastic compression can activate reactive mixtures. A systematic analysis of this problem is necessary to explain the experimental observations and direct experimentalists to systems which are likely to exhibit these phenomena. In this article, we present an analysis of the solid phase chemo-thermoelastic problem. The thermoelastic equation is derived from a linear relation between stress and strain—a constitutive relationship that is violated when strain exceeds a yield limit, but the advantage lies in the simplicity and the preservation of the qualitative behavior. While mechanical inertia does not play any role in typical SHS reactions, because there is a huge disparity between the characteristic times for combustion front propagation and mechanical perturbations, it is included in this analysis. The energy balance includes thermal inertia and the contribution of heating by strain rate. The activation energy depends on both temperature and strain, as suggested by Benderskii et al. The problem is analyzed for the special case of 1-D constant pattern propagation. This assumption negates the stabilizing effects of wave interaction with reaction front in an oscillatory way, as postulated for gaseous detonations (Toong, 1983). The effects of thermal inertia and thermal expansion are investigated. It is shown that the multiplicity changes when these parameters are varied. The analysis also provides guidelines to distinguish between conventional SHS reactions and deflagrations; this is especially helpful for systems which consist of ultrafine powders where the velocities of the two regimes can become of the same order.

Mathematical Model

Consider a mixture of reactive powders, pressed into the shape of a cylinder. It is assumed that the walls of the cylinder are adiabatic and a 1-D description of the system, coinciding with the axial variable of the cylinder used. The mixture is strongly exothermic and in addition to the customary assumption of axial heat conduction, hyperbolic heat transfer is also included. The stress tensor is limited to the axial component, and it is assumed that the angular and radial stresses are negligible. This assumption becomes contentious when radial heat losses occur (Thiart et al., 1993) or thermal expansion is contained in the radial direction.

The displacement of a point (x, y, z) in a continuum to the point $(x + u, y + v, z + w)$ when it is subject to stress, is determined by the displacement equations. We only consider propagation along the z-axis of an isotropic cylinder with adiabatic walls. The displacement equation is

$$(\lambda+2\mu)\frac{\partial^2 u}{\partial z^2}-(3\lambda+2\mu)\alpha_T\frac{\partial T}{\partial z}=\rho\frac{\partial^2 u}{\partial t^2} \tag{1}$$

It is tacitly assumed that the system is adequately described by a linear elastic constitutive relation. Thermal stresses are also included in the displacement formulation. The energy balance accounts for the finite propagation of thermal waves and is given by

$$\left[t_H\frac{\partial}{\partial t}+1\right]\left[\rho C_v\frac{\partial T}{\partial t}+(3\lambda+2\mu)\alpha_T T\frac{\partial^2 u}{\partial z\partial t}-Ck_o(-\Delta H)e^{-(E/RT)}\right]=k\frac{\partial^2 T}{\partial z^2}. \tag{2}$$

The concentration balance is

$$\frac{\partial C}{\partial t}=-k_o Ce^{-(E/RT)}. \tag{3}$$

When the combustion front propagates at a constant speed V (m/s), the coordinate system is translated to the reaction front by introducing

$$\xi=z-Vt. \tag{4}$$

This assumption eliminates other propagation modes, such as oscillatory propagation or chaotic propagation.

In the translated coordinate system, the steady-state displacement equation becomes

$$(\lambda+2\mu)\frac{d^2 u}{d\xi^2}-(3\lambda+2\mu)\alpha_T\frac{dT}{d\xi}=\rho V^2\frac{d^2 u}{d\xi^2}. \tag{5}$$

The term on the righthand side describes inertia. When V is small as is typically the case for SHS propagation, the term is negligible and quasi-steady-state approximation can be used. Boley and Weiner (1960) offered an excellent exposition on the inclusion of inertia, based on the characteristic times for acoustic perturbations and thermal processes. In deflagration and detonation of mixtures, the inertia term plays an important role. Equation 5 can be integrated once to give

$$(3\lambda+2\mu)\alpha_T(T-T_o)=(\lambda+2\mu-\rho V^2)\frac{du}{d\xi}. \tag{6}$$

Use was made of the boundary conditions

$$T\to T_o \qquad \xi\to\infty$$
$$\epsilon=\frac{du}{d\xi}\to 0 \qquad \xi\to\infty.$$

The strain rate becomes $V(d^2u/d\xi^2)$, and it follows from Eq. 5 that the strain rate can be written in terms of temperature. The energy balance becomes

$$\left[-t_H V\frac{d}{d\xi}+1\right]\left[-\rho C_v V\frac{dT}{d\xi}-\left[\frac{(3\lambda+2\mu)^2\alpha_T^2 VT}{\lambda+2\mu-\rho V^2}\right]\frac{dT}{d\xi}-(-\Delta H)Ck_o e^{-(E/RT)}\right]=k\frac{d^2T}{d\xi^2} \tag{7}$$

The Arrhenius form of the reaction rate differs from classical descriptions. Reactants behave quite differently in the solid state. In studies done by Enikolopyan et al. (1991), it was found that intense compressive loading of the specimen changes the activation energy, lowering it with an amount that is proportional to the elastic potential energy. The following relation was proposed (cf. Knyazeva and Dyukarev (1995), Eq. 5)

$$E=E_o+\frac{KM_m\sigma_{\xi\xi}(-\epsilon_{\xi\xi})}{\rho} \tag{8}$$

where K denotes a dimensionless sensitivity factor, M_m is the molar mass (kg/mol), $\sigma_{\xi\xi}$ is the axial stress, and $\epsilon_{\xi\xi}$ is the axial strain. The product of the last two components provides the elastic potential energy of the system

$$(-\epsilon_{\xi\xi})\sigma_{\xi\xi}=\left[-\frac{du}{d\xi}\right]\left[(\lambda+2\mu)\frac{du}{d\xi}-(3\lambda+2\mu)\alpha_T(T-T_o)\right].$$

Define the following dimensionless parameters

$$M=\frac{V}{\sqrt{\frac{\lambda+2\mu}{\rho}}},\quad \delta_s=\frac{t_H(\lambda+2\mu)}{\kappa\rho},\quad \tau_1=\frac{KM_m(\lambda+2\mu)}{\rho E_o},$$
$$\pi_2=\frac{KM_m(3\lambda+2\mu)\alpha_T(T_b-T_o)}{\rho E_o},\quad \alpha_1=\frac{(3\lambda+2\mu)\alpha_T}{\rho C_v},$$
$$\alpha_2=\frac{(3\lambda+2\mu)\alpha_T(T_b-T_o)}{(\lambda+2\mu)},\quad Da=\frac{k_o\kappa\rho e^{-\gamma}}{M^2(\lambda+2\mu)},$$
$$\sigma=\frac{T_o}{T_b-T_o},\quad \gamma=\frac{E_o}{RT_b},\quad \beta=\frac{T_a-T_o}{T_b-T_o}$$

where κ denotes thermal diffusivity ($k/\rho C_v$), T_b and T_a are the combustion and adiabatic temperatures (K), and T_o denotes the far upstream temperature. The temperature, concentration and ξ are scaled as $c=C/C_o$, $\theta=(T-T_o)/(T_b-T_o)$, $s=\xi V/\kappa$.

The two parameters V and T_b which are used in scaling, are not known *a priori*. The Mach number is the ratio of combustion front velocity to longitudinal wave speed and δ_s scales the propagation velocity with thermal diffusivity and the finite thermal wave speed. The parameters π_1 and π_2 relate the mechanical elastic stiffness and thermoelastic stiffness with the activation energy. When α_1 is multiplied with $(\lambda+2\mu)/(3\lambda+2\mu)$, one obtains the Gruneisen parameter at standard conditions. The Damköhler number also contains the Mach number and is the ratio between the reaction and conduction characteristic times. γ is the dimensionless acti-

vation energy parameter, and β is the ratio of adiabatic temperature rise to the temperature rise in the reaction. In the case of very slow propagation speeds, β will be unity.

In dimensionless form, the governing equations can be written as

$$\left[1-\delta_s M^2\frac{d}{ds}\right]\left[-\frac{d\theta}{ds}-\alpha_1\alpha_2\frac{(\theta+\sigma)}{1-M^2}\frac{d\theta}{ds}\right.$$
$$\left.-\beta Da\,ce^{\gamma\left[\frac{\theta-1}{\theta+\sigma}+\frac{(1+\sigma)\pi_2^2M^2\theta^2}{(\theta+\sigma)\pi_1(1-M^2)^2}\right]}\right]=\frac{d^2\theta}{ds^2} \quad (9)$$

$$\frac{dc}{ds}=Da\,ce^{\gamma\left[\frac{\theta-1}{\theta+\sigma}+\frac{(1+\sigma)\pi_2^2M^2\theta^2}{(\theta+\sigma)\pi_1(1-M^2)^2}\right]} \quad (10)$$

with boundary conditions

$$\theta=c-1=0, \quad s\to\infty \quad (11)$$

$$\frac{d\theta}{ds}=c=0, \quad s\to-\infty. \quad (12)$$

It is also assumed that the reaction is limited to a thin section, because the activation energy is high. In the reaction zone the system is both thermally and mechanically activated, and the reaction rate is assumed to be so fast that complete conversion occurs in this section. The reaction zone is located at $s=0$. In Figure 1 the system is presented. The wave propagates from left to right. The temperature remains constant behind the front, and the concentration of the limiting reactant(s) is zero. Since the front propagates at a constant speed, a balance exists between energy released and energy removed over the reaction zone. This will also provide us with a further relationship between the combustion temperature and the propagation velocity.

Outside the reaction zone, the reaction term is neglected in Eqs. 9 and 10. The solution ahead of the front can then be found exactly (albeit in implicit form)

$$s=\frac{d}{b}\ln\frac{\theta(b+a)}{b+a\theta}+2\delta_s M^2\ln\frac{(b+a\theta)}{b+a} \quad (13)$$

where

$$d=-1+\delta_s M^2\left[1+\frac{\alpha_1\alpha_2\sigma}{1-M^2}\right]$$

$$a=\frac{\alpha_1\alpha_2}{2(1-M^2)}$$

$$b=1+\frac{\alpha_1\alpha_2\sigma}{1-M^2}.$$

where a, b, and d are dimensionless factors. The solution to the concentration (C/C_o) balance is

$$c=1, \quad s>0 \quad (14)$$

$$c=0, \quad s<0. \quad (15)$$

Behind the front, the temperature remains constant

$$\theta=1. \quad (16)$$

Remark: A rarefraction wave relaxes the compressed state if the far upstream condition is stress free. The distance between the position of the rarefraction wave and the front continues to increase with time in the supersonic case, since $V>\sqrt{(\lambda+2\mu)/\rho}$.

The reaction zone is analyzed by stretching the variable s as follows; $v=\gamma s$. Also, the dependent variables θ and c and the parameter Da are expressed as perturbation series in terms of $1/\gamma$, that is,

$$\theta=\theta_0+\frac{1}{\gamma}\theta_1+\ldots$$

$$c=c_0+\frac{1}{\gamma}c_1+\ldots$$

$$Da=\gamma Da_0+\ldots$$

where the subscript denotes the ith term of the expansion. When these forms are substituted in Eqs. 9–10 and terms of the same order are collected, one finds for $O(1)$

$$\left[1-\delta_s M^2\left(1+\frac{\alpha_1\alpha_2\sigma}{1-M^2}\right)\right]\frac{d^2\theta_0}{dv^2}-\frac{\delta_s M^2\alpha_1\alpha_2}{1-M^2}\frac{d}{dv}\left(\theta_0\frac{d\theta_0}{dv}\right)$$
$$=\delta_s M^2\left[\beta\frac{d^2c_0}{dv^2}\right] \quad (17)$$

This equation is integrated from $v\to-\infty$ to $v\to+\infty$ and matched with the temperature solution outside the reaction zone.

This outer solution can also be expanded in terms of the perturbation parameter and the expanded variable v. Specifically, for the temperature solution one obtains

$$\theta=1+\frac{1}{\gamma}\frac{b+a}{d+2\delta_s M^2 a}v+\ldots \quad s>0$$

$$\theta=1, \quad s<0$$

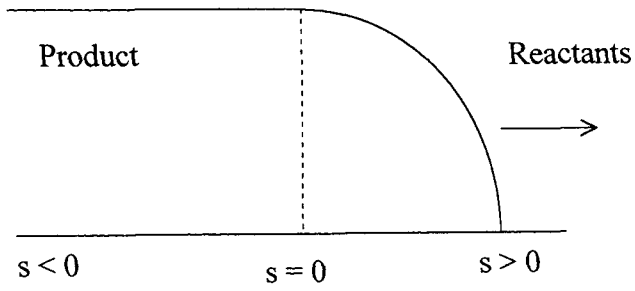

Figure 1. Combustion system.

It follows from Eqs. 14–15 that the derivative dc_0/dv vanishes when $v \to \pm\infty$, hence, the integral of the righthand side of Eq. 17 is zero. The integral of the lefthand side of Eq. 17 is

$$\left[1-\delta_s M^2\left(1+\frac{\alpha_1\alpha_2\sigma}{1-M^2}\right)\right]\frac{d\theta_0}{dv}\bigg|_{-\infty}^{+\infty}-\frac{\delta_s M^2\alpha_1\alpha_2}{1-M^2}\theta_0\frac{d\theta_0}{dv}\bigg|_{-\infty}^{+\infty}=0.$$

Since the leading terms of the outer solutions are 1, they match with the inner solution when $\theta_0 = 1$. The next order terms of the inner expansion are

$$\left[1-\delta_s M^2\left(1+\frac{\alpha_1\alpha_2\sigma}{1-M^2}\right)\right]\frac{d^2\theta_1}{dv^2} = \left[\beta Da_0 c_0 e^{\gamma\frac{\pi_2^2 M^2}{\pi_1(1-M^2)^2}} e^{\theta_1\left(\frac{\pi_1(1-M^2)^2+\pi_2^2M^2(1+2\sigma)}{\pi_1(1-M^2)^2(1+\sigma)}\right)}\right] \tag{18}$$

$$\frac{dc_0}{dv} = Da_0 c_0 e^{\gamma\frac{\pi_2^2 M^2}{\pi_1(1-M^2)^2}} e^{\theta_1\left(\frac{\pi_1(1-M^2)^2+\pi_2^2M^2(1+2\sigma)}{\pi_1(1-M^2)^2(1+\sigma)}\right)}. \tag{19}$$

When the reaction term in Eq. 18 is substituted with dc_0/dv from Eq. 19, it can be integrated from $v \to -\infty$ to v; the following relationship is found between c_0 and $d\theta_1/dv$

$$\left[1-\delta_s M^2\left(1+\frac{\alpha_1\alpha_2\sigma}{1-M^2}\right)\right]\frac{d\theta_0}{dv} = \beta c_0. \tag{20}$$

When the lefthand side of Eq. 20 is substituted for βc_0 in the reaction term of Eq. 18, the resulting equation can be integrated between $v \to -\infty$ to $v \to +\infty$ and matched with $d\theta/dv$ of the outer solution of $O(1/\gamma)$. The following jump condition is found upon reverting from v back to s

$$\left[\frac{d\theta}{ds}\right]+\frac{1}{\gamma}Da\frac{1+\sigma}{1+\dfrac{(1+2\sigma)\pi_2^2M^2}{\pi_1(1-M^2)^2}}e^{\frac{\gamma\pi_2^2M^2}{\pi_1(1-M^2)^2}}=0. \tag{21}$$

The concentration balance has a discontinuity across the front

$$[c] = -1, \tag{22}$$

but the temperature is continuous across the front

$$[\theta] = 0. \tag{23}$$

Note: $[f]$ is defined as $f(0^+) - f(0^-)$.

Discussion of Model

The combustion temperature is given by an overall energy balance of the system. When the reaction term (righthand side of Eq. 10) is substituted by dc/ds in Eq. 9 and integrated from $+\infty$ to $-\infty$ it follows that

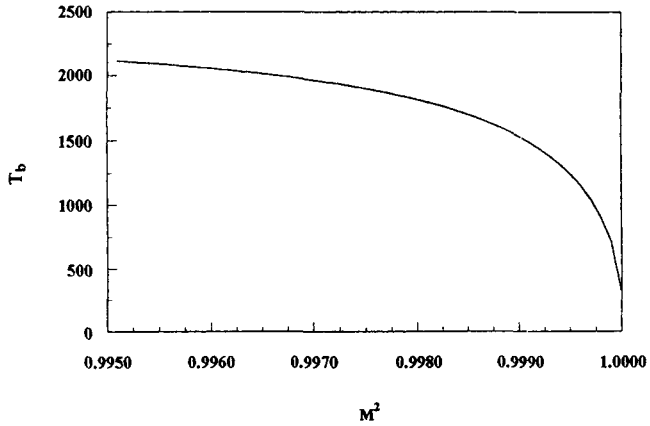

Figure 2. Combustion temperature for subsonic velocities.

$$\beta = 1+\alpha_1\alpha_2\frac{\sigma+0.5}{1-M^2}. \tag{24}$$

Substituting the definitions for the dimensionless numbers in Eq. 24 leads to the following quadratic equation in T_b

$$(1-M^2)(T_a-T_b) = (T_b^2-T_o^2)\frac{(3\lambda+2\mu)^2\alpha_T^2}{(\lambda+2\mu)\rho C_v}. \tag{25}$$

If the Mach number is varied between 0 and values larger than one, two real roots exist as long as the discriminant is positive. The range of real roots is drastically reduced by increased thermal expansion coefficients. Since M also decreases the discriminant as it is increased, real solutions cease to exist for higher Mach numbers. When $M < 1$, only one root is positive and it is plotted in Figure 2 for $\lambda = 2\times10^9$, $\mu = 7\times10^8$, $\rho = 3{,}000$, $C_v = 800$, $T_a = 1{,}800$ and $\alpha_T = 10^{-4}$ (all SI units). When $M > 1$, there is a small region near $M = 1$ where the discriminant is negative. Both roots are positive outside this region, but one of the roots goes to unrealistic large values, and the other root approaches the adiabatic temperature as M increases. In Figure 3 this latter root is shown for $M > 1$ (all parameters the same as for Figure 2). In

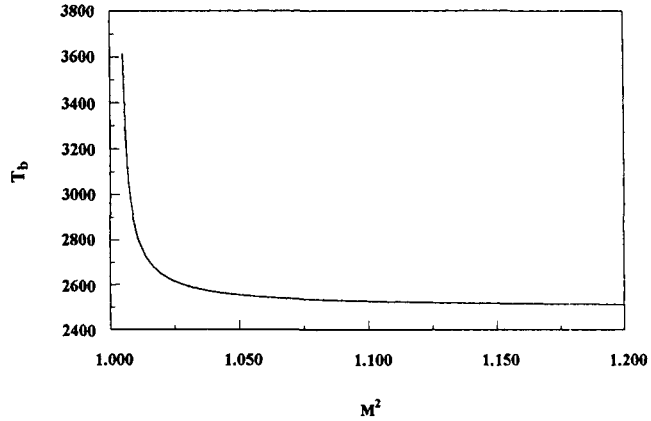

Figure 3. Combustion temperature for supersonic velocities.

summary, one can use Eq. 25 to write T_b as a function of the Mach number

$$T_b = f_1(M).$$

The second aspect, which must be considered in determining the domain of Mach numbers which contains feasible solutions, is the change in the activation energy. The activation energy depends on Mach number as given by Eq. 8, but it can only vary between $0 \le E \le E_o$. This leads to the inequality

$$\pi_1(1 - M^2) \ge \pi_2^2 M^2. \tag{26}$$

The parameters π_1 and π_2 can be written in terms of their physical parameters and T_b can be substituted with $f_1(M)$. The inequality demarcates a region around $M = 1$, where the solutions cannot exist. The term domain of solution will be used to refer to that set of M values where the inequality (Eq. 26) holds. In Figure 4 the domain of the solution is shown for two different adiabatic temperatures and $\alpha_T = 8 \times 10^{-5}$ K^{-1}; other parameters have the same values as used in Figure 2. When $T_a = 2{,}500$ K, a small region around $M = 1$ is excluded from the solution domain, when T_a is increased to 3,000 K, the region where no solutions exists, is increased. Both higher adiabatic temperatures and higher thermal expansion coefficients decrease the domain of solvability.

A solution exists when the jump condition stated in Eq. 21 is satisfied within the domain of solution. The slow combustion solution is also found by solving Eq. 21 in the domain of solution. However, the fact that the Mach number is small can be exploited to find an explicit expression for the Mach number. The Mach number is expanded as a perturbation series in terms of the small parameter ϵ, that is, $M = \epsilon M_1 + \epsilon^2 M_2 + \ldots$, and substituted into Eq. 21. The term $[d\theta/ds]$ in Eq. 21 is evaluated from Eq. 13. Correct to $O(\epsilon)$, the Mach number is found to be

$$M_1 = \sqrt{\frac{RT_b k_o \kappa \rho e^{-\gamma}(1+\sigma)}{E(\lambda+2\mu)[1+\alpha_1\alpha_2(0.5+\sigma)]}}. \tag{27}$$

The result differs from the classical result of Novozhilov (1961), because the strain rate is included in the energy balance. It must be added that this contribution to the Mach number is very small in this case.

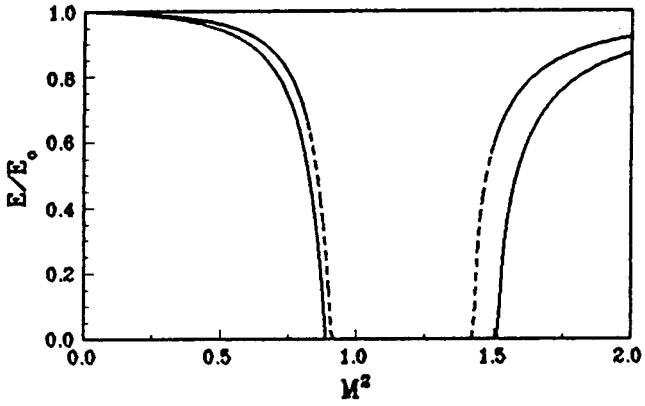

Figure 4. Domain of feasible solutions for $T_a = 2{,}500$ K (---) and $T_a = 3{,}000$ K.

Results

The longitudinal sound velocity in an isotropic solid medium is given by

$$V_L = \sqrt{\frac{\lambda + 2\mu}{\rho}}.$$

Data for stiffness constants and densities are readily available for a wide range of ceramics, metals, alloys and other materials. The sound velocity in a solid-solid reacting system depends on the type of powders and the method in which the preform was prepared. To illustrate this point, consider a mixture with a Poisson ratio of 0.25 (this choice sets the two Lame constants equal) and a density of 3,000 kg/m^3. The sound velocity varies from 40 m/s at $\lambda = 1.6$ MPa to 2,000 m/s at $\lambda = 4$ GPa. The elastic properties of premixed powders pressed in a preform depend on the powder's properties, the pressure applied in the preform and binding agents. Therefore the sound velocity depends on two factors: the choice of material and the preparation of specimens.

Data for the hyperbolic coefficient δ_s is practically nonexistent. With the growing applications of lasers in materials, the need for physical data will increase and experimental results will become available to augment the numerical studies. Another parameter we have no published information on is the sensitivity constant K (cf. Eq. 8). Shlensky (1995) gave an insightful discussion of the sensitivity of an explosive material and the relation to homogeneous nucleation. Lack of available data forces us to use estimated values as listed in Table 1, which are typical for thermite systems.

For the first example, we choose an activation energy (J/mol), $E_0 = 2.5 \times 10^5$, $k_0 = 10^{10}$, and $\alpha_T = 10^{-4}$. The values of the other properties are in Table 1. The sound velocity for this example is 1,065 m/s. A thermite solution (typical SHS) exists at a propagation velocity of 0.028 m/s. The combustion temperature $T_b = 1{,}800$ K is the same as the adiabatic value. However, another solution can be found. This second solution has a Mach number $M = 0.966$, and the combustion temperature is only 958 K. The solution is similar to the results observed by Enikolopyan et al. (1991). The activation energy is significantly reduced in the reaction front, and the propagation velocity is 1,028.4 m/s. Evidently, it is a solution that

Table 1. Parameter Values

Property	Value	Units
M_m	0.045	kg/mol
λ	2.0×10^9	Pa
μ	7.0×10^8	Pa
ρ	3,000.0	kg/m^3
C_v	800	J/(kg·K)
t_H	1.0×10^{-11}	s
k	50.0	W/(m·K)
T_o	300	K
E_o	1.0×10^5	J/mol
k_o	1.0×10^{14}	s^{-1}
α_T	2.0×10^{-4}	K^{-1}

belongs to the fast deflagration SHS regime. For these parameters, the detonation solution does not exist. This behavior corresponds qualitatively with the system $Mg + S \rightarrow MgS$.

For systems featuring higher reaction rates, the detonation SHS regime can be predicted. (Reaction rates are significantly faster when ultrafine powders are used, cf. Batsanov (1996).) In order to find a supersonic solution, it is necessary to increase the frequency factor k_o (s^{-1}); we also consider a lower activation energy. When k_o is set to 10^{14} and $E_0 = 10^5$ and other parameters as listed in Table 1, three combustion solutions are found: a slow deflagration, a fast deflagration, and a detonation. However, the slow deflagration in this case becomes fast, compared to traditional values. The slow deflagration has a velocity of 285.7 m/s and temperature $T_b =$ 1,492. This velocity is typical for ultrafine powders which are mixed on the "micronano level." The second solution is a fast deflagration with a propagation velocity of 919 m/s and $T_b =$ 1,151 K. The third solution is of the SHS detonation type, propagating at 1,684 m/s and a combustion temperature of 2,242 K. The temperature in the front is superadiabatic while the velocity is relatively low for SHS detonation.

In Figure 5a the temperature profiles for the slow deflagration and fast deflagration are shown. The reader is reminded that both s and θ are scaled differently for each solution. The detonation solution propagates so fast that the temperature profile in the preheating zone takes on wave-like character; note the discontinuity in the temperature shown in Figure 5b. The length scale is much shorter than for the other two solutions, and significant gradients exist on the 100 Å mesh which is typical for high power detonation.

The multiplicity behavior of the system is illustrated in Figures 6a–6c. The thermal expansion parameter α_T (K^{-1}) is the bifurcation parameter. In Figure 6a the velocities are plotted vs. α_T for the slow deflagration, fast deflagration and detonation solutions. The detonation solution reaches velocities of 2,887 m/s when α_T is 5×10^{-4}. A typical detonation velocity for exothermic solid-solid reactions is in the range of 4–10 km/s; it is evident that this range is approached if the thermal expansion coefficient is increased. The solution branch of the fast deflagration solution has a limit point at $\alpha_T = 2.04\times10^{-4}$. A more detailed plot is shown in Figure 6b. The upper branch terminates at $\alpha_T = 1.98\times10^{-4}$ when it reaches the end of the domain of solutions (cf. inequality (Eq. 27)). The temperatures of the three different solutions are shown in Figure 6c. The temperature of the detonation SHS solution increases to values of 2,890 K, compared to the adiabatic value of 1,800 K. The fast deflagration temperature is subadiabatic, and the temperature at the limit point is 926 K. Although the three different solution branches are not connected (ruling out conventional continuation methods), because there is a singularity at $M = 1$ and the region around $M = 1$ is excluded from the domain of solution, it appears that all three solution branches approach the adiabatic temperature at small values of α_T. The interesting result is that the temperature for the slow deflagration is higher than the temperature for the fast deflagration.

Remark: There is also a slow-reacting kinetic solution for the problem that has been ignored in this analysis.

In the next study δ_s is used as the bifurcation parameter. In Figure 7a the velocities of the fast deflagration and detonation are plotted as a function of $\delta_s/10^{-11}$. The detonation SHS solution branch is terminated at $\delta_S = 1.9\times10^{-11}$; at this value, the discontinuity of the thermal wave coincides with the reaction front. When $\delta_S = 0$, the parabolic temperature form is recovered and the velocity reaches a maximum. The fast deflagration solution exhibits the opposite behavior. The velocity increases with increasing values of δ_s. The solution branch also terminates at 1.02×10^{-11} when the reaction front and thermal wave coincide. The velocity at $\delta_s = 0$ is 871 m/s. In Figure 7b the slow deflagration solution branch is shown. The velocity decreases when δ_s increases. The solution branch is not terminated at larger δ_s values, because the front does not travel fast enough to overtake the thermal wave. The maximum velocity is attained at $\delta_s = 0$.

To summarize, the fast deflagration and detonation solutions are very sensitive to the value of δ_s and disappear when δ_s becomes larger, but the slow deflagration solution is rather insensitive to δ_s. The consequence for practical systems is the possible absence of fast deflagration or detonation solutions. The lack of information on δ_s makes the problem more vexing. The temperatures are plotted in Figure 7c for the fast deflagration and detonation solutions. Opposite trends are observed for the two regimes. The detonation temperature increases when δ_s increases and the maximum temperature

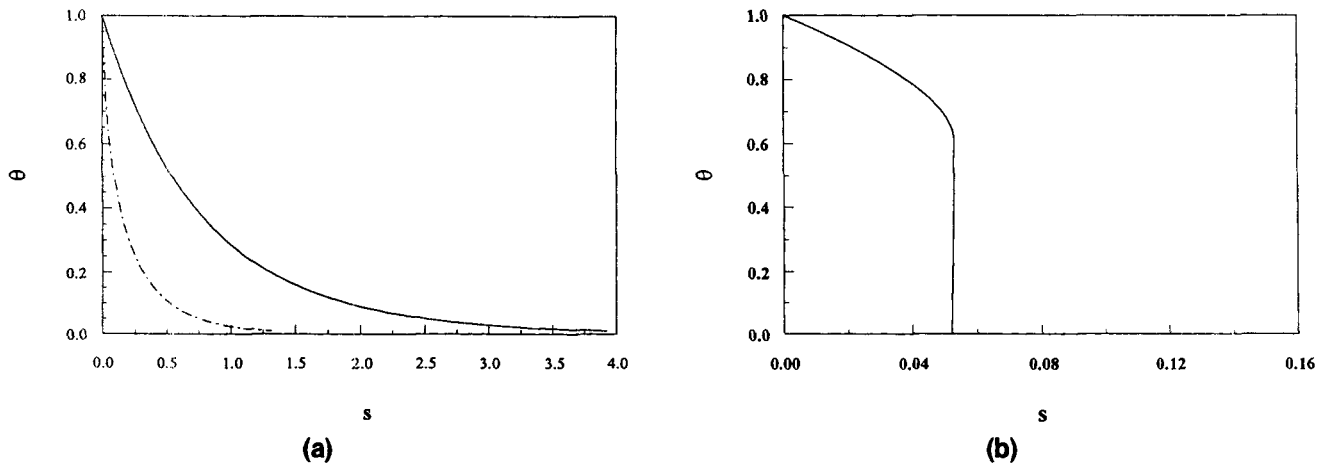

Figure 5. Temperature profiles in the preheating zone: (a) slow and fast (---) deflagrations; (b) for detonation.

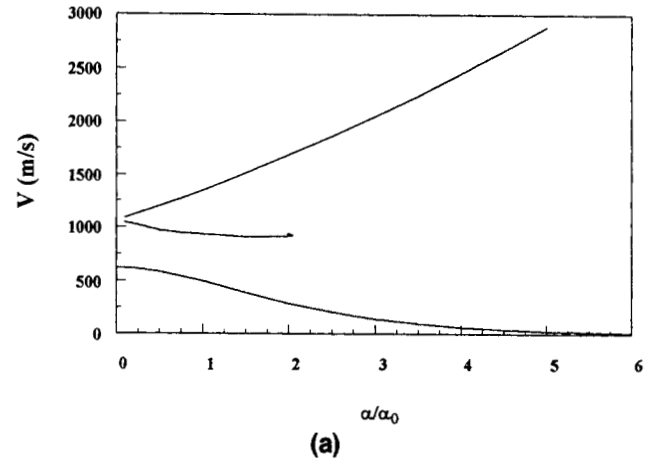

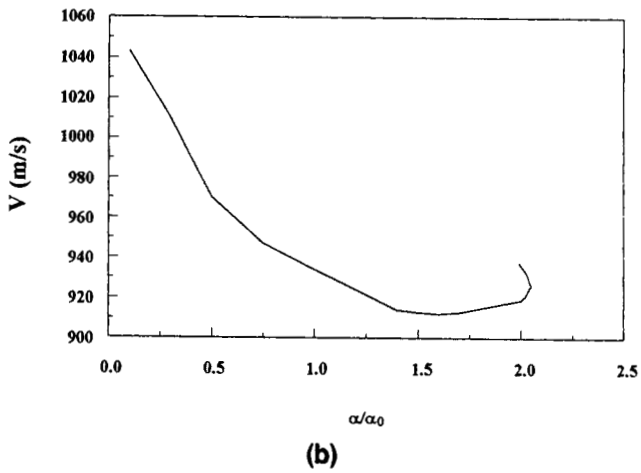

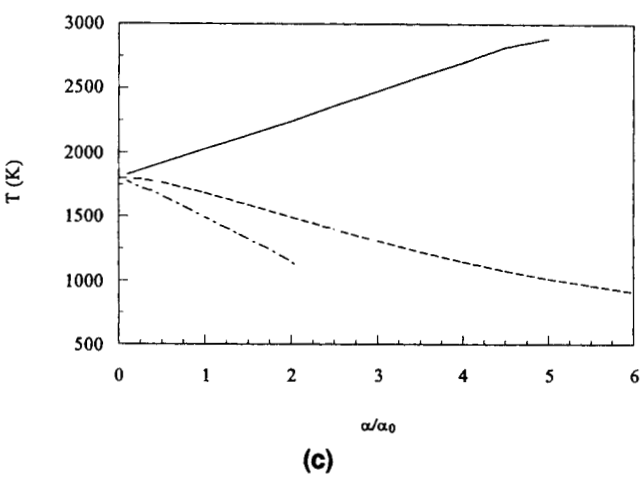

Figure 6. (a) Velocity vs. $\alpha_T/10^{-4}$ for different solutions; (b) velocities of fast deflagration regime vs. $\alpha_T/10^{-4}$; (c) temperature vs. $\alpha_T/10^{-4}$ for different solutions.

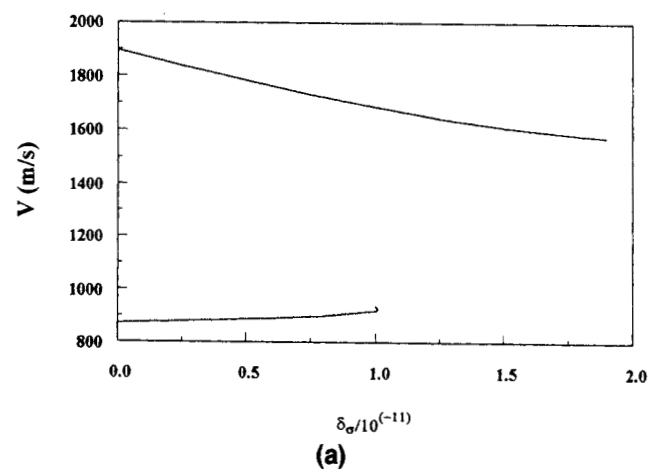

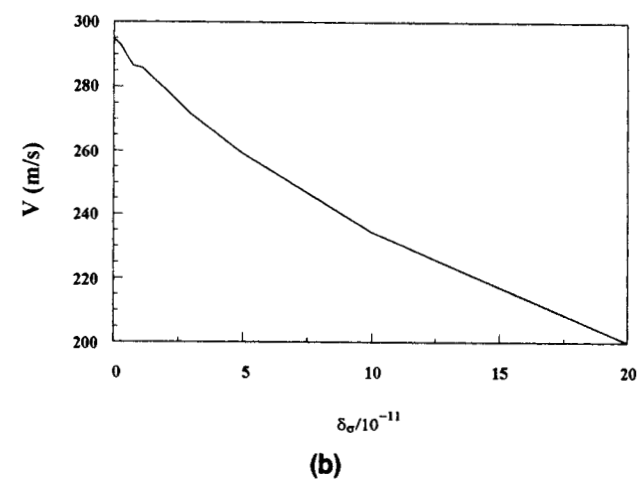

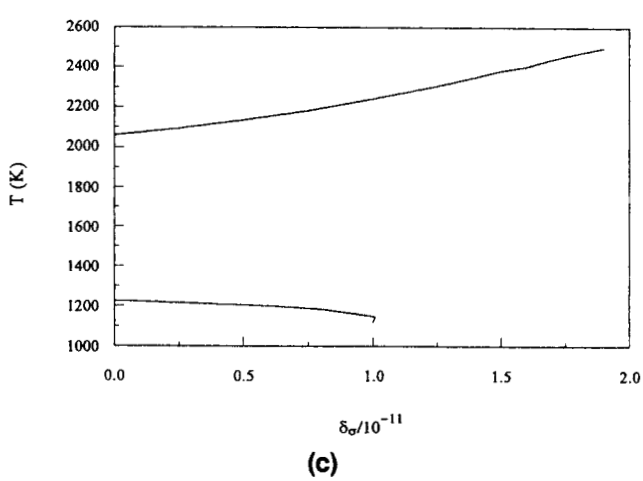

Figure 7. (a) Velocity vs. $\delta_s/10^{-11}$ for different solutions; (b) slow deflagration velocity vs. $\delta_s/10^{-11}$; (c) fast deflagration and detonation temperatures vs. $\delta_s/10^{-11}$.

of the fast deflagration is reached at $\delta_s = 0$. The temperature of the slow deflagration is insensitive to δ_s and vary only by 10 K over the span of δ_s values. As expected, thermal wave behavior disappears at slow propagation velocities.

Discussion

Under certain conditions, the solid-solid reactions can exhibit interesting multiplicity, namely slow deflagration, and two fast deflagration solutions as well as detonation. The in-

dividual regimes require different ways of initiation (ignition, shock waves). The model formulated here describes both deflagration and detonation regimes, as well as Enikolopyan's low exothermicity explosions. There are compelling arguments to include more complex features into future models. In the following discussion, which is incomplete, we list aspects which should be addressed in the future.

- It would be an oversimplification to assume that the same kinetic parameters E_o and k_o hold for both the slow thermite solution (SHS mode) and the fast reactions in the compressed state. In an article by Rode et al. (1992) the oxidation of *Al* was studied. Different processes control the rate of reaction at different stages of the oxidation process. For example, when the oxide layer has just formed, electron tunneling is the dominant process, followed by cation convection as the film gets slightly thicker. When the film grows to thicknesses that weakens the electric field, cation diffusion becomes the rate controlling step. Each one of these processes has different kinetic parameters.
- Evidently, a wide spectrum of solutions can exist which can even exhibit dynamic features in a Lagrangian description, such as planar oscillating waves, 2-D and 3-D rotating waves, cellular structures, and nonperiodic modes. The analysis must be expanded to 2-D and 3-D to capture all features which are present in experiments. The consideration of stress and strain components in the other directions can introduce shear in the systems; an important effect that was already demonstrated by Enikolopyan's experiments. Destabilization of the front by a symmetry-breaking bifurcation in directions normal to the front is masked by a 1-D description.
- The displacement Eq. 1 is derived from the linear constitutive relation

$$\sigma = c\epsilon$$

where σ and ϵ are the stress and strain tensors and c is the stiffness tensor. This relationship can be good for deflagration, however, in the detonation regimes pressures up to 10^6 atm exist which require a more sophisticated description. Ahrens (1993) suggested that an equation of state be used for porous materials, based on the Mie-Gruneisen relation. This nonlinear equation of state can account for anomalous behavior of porous powders where the volume increases with compressive loading. Evidently, including the elastoplastic properties of the continuum in the model and the resulting spectrum of deflagration-detonation phenomena represents an interesting modification of the conventional models of solid-solid SHS operations. Under mechanical load of a solid, the system acquires energy in two different processes: elastic and plastic deformation. The elastic potential energy results in the distortion of interatomic distances and bond angles and chemical reactions take place without or with small activation barrier, and therefore the reactions become independent or weakly dependent on temperature. Plastic deformation is an irreversible process and the energy is used to form new surfaces, breaking intermolecular and interatomic bonds and creates surface defects, radicals, ions, and so on in the solid.
- When materials are compressed to high pressure, intimate contact exists between the solid reactants. In the presence of high temperature sintering can occur, and a densification of the compact can result. This can have both favorable and negative effects on the reaction rate. Ramqvist (1966) gives a survey of models for the hot-pressing of powders. The rate of densification expressions are given, which correlate well with experimental results. These expressions can be considered as equations of state and should be integrated with equations of state like Gruneisen or Birch-Murnaghan.
- A criterion along similar vein as the Griffith's criterion (Cherepanov, 1979) is necessary to make provision for crack formation. A short discussion, based on heuristic arguments, is in order. When microcracks form, their presence is reflected in the adjustment of the stiffness constants (cf. Walsh, 1965). These cracks must be small enough to prevent the destabilization of the planar front. The lowered values of the Lame constants lead to a reduction in the propagation velocity. But, the material on the crack surface is at a higher energy state and the activation energy would be lower; this should increase the propagation velocity. These opposing effects complicate *a priori* deductions. There exists convincing experimental evidence that cracks propagate at speeds between $^1/_2V_L$ and $^2/_3V_L$. Therefore, reaction driven cracking cannot play a role in supersonic combustion. But, it can coexist with deflagration propagation and plays a causal role in destabilizing the latter state to progress from a deflagration to a detonation.
- There is a potential flaw in the argument that the shock wave and the reaction wave propagate at the same speed. Numerical studies with systems defined in laboratory coordinates can elucidate this point.
- There is a lack of physical data for these systems. Experiments are needed to measure thermal and mechanical properties of compressed reactant powders. Kinetic data would be difficult to collect in the conventional way, however, measurements of wave propagation velocities and observation of quality of pattern formation in the fronts can result in improved values of the governing parameters.
- The results suggest that under certain conditions, the molecular mixing and chemical transformation processes in solids take place at rates which exceed the relaxation rates for elastic deformation. To achieve such extremely high reaction rates, diffusion should be absent. In other words, the precursors must be extremely fine and in addition, must be mixed at almost the molecular level. There must be a mechanism which allows the ultrafast interaction of atoms. Batsanov (1996) proposed a very interesting idea to explain the fast mass transfer. His mechanism suggests that ultrarapid diffusion is caused by a difference in the particle velocities of components of a heterogeneous mixture. These differences are caused by different compressibility of individual components participating in the reaction.

Notation

C = concentration, mol/m^3
C_v = specific heat capacity at constant strain, J/kg·K
G = surface energy, J/cm^2
$-\Delta H$ = heat of reaction, J/mol
R_g = universal gas constant, J/mol·K
$s = \xi V/\kappa$
t = time, s
t_H = thermal inertia coefficient, s
u = displacement vector, m
$\delta = \delta_s M^2$
λ = Lame constant, Pa

μ = Lame constant, Pa
$\pi_1 = [KM_m(\lambda + 2\mu)]/\rho E_o$
$\pi_2 = [KM_m(3\lambda + 2\mu)\alpha_T(T_b - T_o)]/\rho E_o$
ρ = density, kg/m^3

Subscripts

a = adiabatic
o = initial

Literature Cited

Ahrens, T. J., "Equation of State," *High-Pressure Shock Compression of Solids*, J. R. Asay and M. Shahinpoor, eds., Springer-Verlag, New York (1993).

Aumann, C. E., G. L. Skofronick, and J. A. Martin, "Oxidation Behavior of Aluminium Nanopowders," *J. Vac. Sci. Tech.*, **B13**(3), 1178 (1995).

Batsanov, S. S., "Solid Phase Reactions in Shock Waves. Kinetic Study and Mechanism," *Comb. Explos. Shock Waves*, **32**(1), 102 (1996).

Benderskii, V. A., P. G. Filippov, and M. A. Ovchinnikov, "Ratio of Thermal and Deformation Ignition in Low-Temperature Solid-Phase Reactions," *Doklady Akad. Nauk SSSR*, **308**(2), 401 (1989).

Benson, D. J., V. F. Nesterenko, and F. Jonsdottir, "Numerical Simulations of Dynamic Compaction," *Proc of the Net Shape Processing of Powder Materials Symp.*, ASME Int. Mech. Eng. Cong. and Exp., San Francisco (1995).

Boley, B. A., "The Analysis of Problems of Heat Conduction and Melting," *High Temperature Structures and Materials*, Pergamon Press, New York (1964).

Boley, B. A., and J. H. Weiner, *Theory of Thermal Stresses*, Wiley, New York (1960).

Cherepanov, G. P., *Mechanics of Brittle Fracture*, McGraw-Hill, New York (1979).

Danen, W. C., and J. A. Martin, "Energetic Composites," U.S. Patent No. 5,266,132 (1993).

Enikolopyan, N. S., "Super-Fast Chemical Reactions in Solids," *Russian J. Phys. Chem.*, **63**(9), 1261 (1989).

Enikolopyan, N. S., et al., "Direct Conversion of Chemical Energy into Mechanical without Thermalization," *Doklady Akad. Nauk SSSR*, **319**(6), 1384 (1991).

Gogulya, M. F., et al., "Interaction of Sulphur and Aluminium Behind Shock Fronts," *Khim. Fiz.*, **10**, 420 (1991).

Gogulya, M. F., et al., "Interaction of Sulphur and Aluminium Behind Shock Fronts," *Khim. Fiz.*, **11**, 224 (1992).

Knyazeva, A. G., "Combustion Wave Propagation Through Deformed Solids," *Combustion, Explosions, and Shock Waves*, **29**(3), 48 (1993).

Knyazeva, A. G., and E. A. Dyukarev, "Stationary Wave of a Chemical Reaction in a Deformable Medium with Finite Relaxation Time of the Heat Flux," *Combustion Explosions and Shock Waves*, **31**(3), 37 (1995).

Knyazeva, A. G., "Hot Spot Thermal Explosion in Deformed Solids," *Combustion Explosions and Shock Waves*, **29**(4), 3 (1993).

Kovalenko, A. V., and G. I. Ivanov, "Physical and Chemical Transformations of Lead Nitrate in Mixtures with Aluminium under Shock Waves," *Comb. Expl. and Shock Waves*, **17**(4), 141 (1981).

Maurer, M. J., and H. A. Thompson, "Non-Fourier Effects at High Heat Flux," *ASME J. Heat Transfer*, **95**, 284 (1973).

Morse, P. M., and H. Feshbach, *Methods of Theoretical Physics I*, McGraw-Hill, New York (1953).

Nesterenko, V. F., et al., "The Structure of Controlled Shear Bands in Dynamically Deformed Reactive Mixtures," *Metall. and Mat. Trans. A*, **26**, 2511 (1995).

Nesterenko, V. F., et al., "Controlled High Rate Localized Shear in Porous Reactive Media," *Appl. Phys. Lett.*, **65**, 3069 (1994).

Novozhilov, B. V., "Velocity of Propagation of the Front of an Exothermic Reaction in a Condensed Medium," *Doklady Akad. Nauk, SSSR*, **141**(1), 151 (1961).

Ramqvist, L., "Theories of Hot Pressing," *Powder Metall.*, **9**, 1 (1966).

Rode, H., et al., "A Phenomenological Model for the Combustion of Ultrafine Powders: Modeling of Pyrophoricit," *Comb. Sci. Tech.*, **88**(3–4), 153 (1992).

Shlensky, O. F., and G. G. Murashov, "Mathematical Modeling of Front Processes of Thermal Decomposition of a Substance with an Accounting for a Finite Velocity of Heat Propagation," *Doklady Akad. Nauk, SSSR*, **269**(6), 1406 (1983).

Shlensky, O. F., "Influence of Homogeneous Nucleation on the Rate of Exothermic Thermal Decomposition of Condensed Systems," *Comb. Expl. and Shock Waves*, **31**(1), 87 (1995).

Sivashinsky, G. I., "On Spinning Propagation of Combustion Waves," *SIAM J. Appl. Math.*, **40**, 432 (1981).

Taylor, T. N., and J. A. Martin, "The Reaction of Vapor Deposited Al with Cu Oxides," *J. Vac. Sci. & Tech.*, **A9**, 1840 (1991).

Thiart, J. J., H. J. Viljoen, J. E. Gatica, and V. Hlavacek, "Thermal Stresses in Combustion Synthesis of Inorganic Materials," *J. Mat. Synthesis and Processing*, **1**(4), 209 (1993).

Toong, T.-Y., *Combustion Dynamics*, McGraw-Hill, New York (1983).

Walsh, J. B., "The Effect of Cracks on the Compressibility of Rock," *J. Geophysical Res.*, **70**, 381 (1965).

Manuscript received Mar. 7, 1997, and revision received June 12, 1997.